Journal of the Association of Arab Universities for Basic and Applied Sciences (2015) 17, 82–89

University of Bahrain
Journal of the Association of Arab Universities for Basic and Applied Sciences
www.elsevier.com/locate/jaaubas
www.sciencedirect.com

المجال الحراري لخلية وقود أُوكسيدية صلبة مغذية بالميثان: تأثير الكسور المولارية للوقود

Abdenebi Hafsia [a,c,*], Zitouni Bariza [a,b,c], Ben Moussa Hocine [a,c], Haddad Djamel [a,c]

[a] Department of Mechanic, Batna, Algeria
[b] Department of Food Technology, Institute of Veterinary Sciences and Agricultural Sciences, Batna, Algeria
[c] Univeriy Hadj Lakhdar, Batna, Algeria

المخلص:

تم خلال العمل الحالي تغذية خلية وقود أُوكسيدية صلبة (AS_SOFC) محملة على الأنود بخليط من الهواء والوقود عند قناتي الكاثود والأنود على التوالي. كان الوقود عبارة عن خليط من خمس مكونات هي: الميثان (CH_4)، الهيدروجين (H_2)، ثاني أوكسيد الكربون (CO_2)، أول أوكسيد الكربون (CO)، والبخار(H_2O)؛ حيث جرت عملية تهذيب داخلية او خارجية. فعند جانب الأنود جرت عملية تهذيب مباشرة أوغير مباشرة. أن الهدف الرئيس من هذه الدراسة هو إلقاء الضوء على مجالات الحرارة عندما تكون تحت تأثير المصادر الحرارية المتولدة من جراء تفاعلات التهذيب الداخلية المباشرة وهي :تفاعل التهذيب البخاري، تفاعل إزاحة الغاز المائي و تفاعل التهذيب الكلي. كما تم تناول تدرجات درجة الحرارة لعدد من الكسور المولارية للوقود الداخل. لهذا الغرض تم تطوير برنامج باستخدام لغة فورتران باستعمال طريقة الفروق المنتهية. تمت قراءة المجالات الحرارية في مستوى متعامد مع سطح سريان الغاز باستعمال برنامج "مخطط تك (Tech plot) . إن هذه الدراسة تتطلب وجود معادلات محافظة وتزاوج بين الكتلة والطاقة والنوع. وقد تم التحكم في سريان الغازات بتطبيق قانون داكري. أوضحت النتائج أن الكسور المولارية للوقود لا يمكن تجاهلها في وجود ظاهرة التهذيب المباشر الداخلي.

Journal of the Association of Arab Universities for Basic and Applied Sciences (2015) **17**, 82–89

University of Bahrain

Journal of the Association of Arab Universities for Basic and Applied Sciences

www.elsevier.com/locate/jaaubas
www.sciencedirect.com

ORIGINAL ARTICLE

Thermal field in SOFC fed by CH_4: Molar fractions effect

Abdenebi Hafsia [a,c,*], Zitouni Bariza [a,b,c], Ben Moussa Hocine [a,c], Haddad Djamel [a,c]

[a] *Department of Mechanic, Batna, Algeria*
[b] *Department of Food Technology, Institute of Veterinary Sciences and Agricultural Sciences, Batna, Algeria*
[c] *Univeriy Hadj Lakhdar, Batna, Algeria*

Received 3 January 2013; revised 31 December 2013; accepted 14 January 2014
Available online 20 February 2014

KEYWORDS

SOFC;
Molar fractions;
Steam reforming;
Shift reaction;
Temperature;
Direct internal reforming

Abstract In the present work, the anode supported solid oxide fuel cell (AS_SOFC) is fed by air and fuel at cathode and at anode channels respectively. The fuel is a mixture of five components: methane (CH_4), hydrogen (H_2), carbon dioxide (CO_2), carbon monoxide (CO) and steam (H_2O), where a reforming phenomenon; an external or an internal one appears. At the SOFC anode side, an indirect or direct reforming phenomenon happens.

The principal aim of this study is the visualization of the temperature fields under heat sources' effect caused by the direct internal reforming reactions; the steam reforming reaction, the water gas shift reaction and the overall reforming reaction. The temperature gradient is discussed for several inlet fuel molar fractions.

A program in FORTRAN language using the finite difference method is developed. The thermal fields', in the plane perpendicular to the gas flow, is visualized by "Tec plot" program. This study requires a coupling conservation equations (mass, energy and species). The flows are governed by Darcy's law. The results show that the fuel molar fractions cannot be ignored in the presence of direct internal reforming phenomenon.

1. Introduction

Demographic growth has encouraged companies to diversify and increase their energy resources. However, this development cannot be accomplished simply by increasing fossil fuel (oil, gas or coal) consumption. Indeed, the energy demand increase associated with resource scarcity currently conducts to oil price increases. This economic problem is accompanied by a major environmental challenge: the use of hydrocarbons generates CO_2 immense emissions that contribute to planet global warming. Therefore, it becomes essential to find alternative concurrently technological solutions to: (i) limit energy consumption, (ii) increase the efficiency of fossil fuel converters into usable energy (electricity and transport) and (iii) develop cleaner sources and energy carriers.

To attain these objectives, it is particularly necessary to develop new energy technologies. Solid oxide fuel cell (SOFC) comes in this context. This technology is indeed the most effective way to convert the hydrocarbon chemical energy into electricity. This transformation takes place at high temperature

* Corresponding author. Tel./fax: +213 33 81 21 43.
E-mail addresses: abdenebihafsa@gmail.com, H2SOFC@gmail.com (H. Abdenebi).

Peer review under responsibility of University of Bahrain.

1815-3852 © 2014 Production and hosting by Elsevier B.V. on behalf of University of Bahrain.
http://dx.doi.org/10.1016/j.jaubas.2014.01.002

(600–1000 °C) on the basis of an electrochemical fuel oxidation and oxygen reduction from the air (Laurencin, 2008). This high temperature has a double advantage. First, it assures the provision of easily exploitable high heat in cogeneration. Secondly, it allows the hydrocarbons direct use, primarily natural gas, which can be easily reformed in order to produce hydrogen for SOFC fuel cell. According to the literature review, when it is fed by a fuel other than hydrogen; CH_4, H_2, CO_2, CO, H_2O, molar fractions do not have the same percentage (Table 1).

The present work's contribution is to study the temperature fields under the heat source effect caused by the direct reforming reactions; the steam reforming reaction, the water gas shift reaction and the overall reforming reaction. The parameter studied is the inlet fuel molar fractions.

2. Physical model

The physical model adopted for the SOFC direct reforming phenomenon simulation is shown in Fig. 1. The first compartment, corresponding to an anode supported planar SOFC fuel cell is fed by fuel and air (Fig. 1(a)). The second one; (Fig. 1(b)) shows the study area. The latter is composed by:

- Two interconnections; anode and cathode interconnections,
- Two electrodes (anode and cathode),
- An electrolyte.

Fig. 1(c) represents the anode, reforming and electrochemical reaction locations, and the anode interconnection. The reactions that occurred in the anode and considered in the mathematic model are:

Reforming reactions:

$$\text{- Steam reforming reaction : } CH_4 + H_2O \rightarrow 3H_2 + CO \quad (1)$$

$$\text{- Water} - \text{gas shift reaction : } CO + H_2O \rightarrow H_2 + CO_2 \quad (2)$$

$$\text{- Overall reforming reaction : } CH_4 + 2H_2O \rightarrow 4H_2 + CO_2 \quad (3)$$

3. Mathematical model

For this numerical study, the planar SOFC is fueled by gases; air and fuel. The fuel is a mixture of methane (CH_4), hydrogen (H_2), carbon monoxide (CO), carbon dioxide (CO_2) and steam (H_2O). Thermal field's visualization is made in the plane perpendicular to the gas flow direction of a single cell (Fig. 1). This study requires coupling conservation equations; mass, energy and species. For the momentum equation in the porous electrodes, the flow is modeled using Darcy's law.

$$U = -\frac{\kappa}{\varepsilon.\mu} grad(p) \quad (4)$$

where 'U' (m s^{-1}) is the velocity, 'κ' (m^2) is the permeability, 'ε' (%) is the porosity, 'μ' (kg m^{-1} s^{-1}) is the viscosity and 'p' (Pa) is the pressure.

The basic equations; mass, energy and species can be written following a general form:

$$div(\varepsilon\rho U\Phi) = div(\Gamma_\Phi grad\Phi) + S_\Phi \quad (5)$$

where 'ρ' (kg m^{-3}) is the density, 'Φ' is a general variable, 'Γ_Φ' (m^2 s^{-1}) is the diffusion coefficient and 'S_Φ' is the source term. Table 2 explains mass, energy and species equations obtained from the Eq. (5).

The fuel used is a gas mixture and based on the ideal gas law:

$$PV = nRT \quad (6)$$

where 'V' (m^3) is the volume occupied by the fuel, 'n' is the moles number, 'R' (kg m^{-1} s^{-1}) is the gas constant and 'T' (K) the temperature. The relation which gives the mole number is:

$$n = \frac{m}{M} \quad (7)$$

where 'm' (kg) and 'M' (kg mol^{-1}) are the mass and the molar mass respectively. As a result, the fuel density 'ρ_{fuel}' can be expressed as (Hamid, 2010):

$$\rho_{fuel} = \frac{P_{fuel}M_{fuel}}{RT} \quad (8)$$

Where 'M_{fuel}' is the fuel molar mass and it is calculated by the following relation (Hamid, 2010).

$$M_{fuel} = \sum_1^5 M_j X_j = M_{CH_4}X_{CH_4} + M_{H_2}X_{H_2} + M_{CO_2}X_{CO_2} + M_{CO}X_{CO} + M_{H_2O}X_{H_2O} \quad (9)$$

Table 1 Molar fractions of components.

Components	Molar fractions	Refs.	Components	Molar fractions	Refs.
CH_4	0.29	Li et al. (2008)	CH_4	0.171	Ferguson et al. (1996), Kang et al. (2009)
H_2	0.09		H_2	0.2626	
CO_2	0.01		CO_2	0.0436	
CO	0.01		CO	0.0294	
H_2O	0.6		H_2O	0.4934	
CH_4	0.1707	Ho et al. (2010)	CH_4	0.33	Kang et al. (2009)
H_2	0.2686		H_2	/	
CO_2	0.0491		CO_2	/	
CO	0.024		CO	/	
H_2O	0.4875		H_2O	0.67	
CH_4	0.171	Wang et al. (2009)	CH_4	0.110	Hu et al. (2008)
H_2	0.263		H_2	0.258	
CO_2	0.044		CO_2	0.228	
CO	0.029		CO	0.057	
H_2O	0.493		H_2O	0.284	

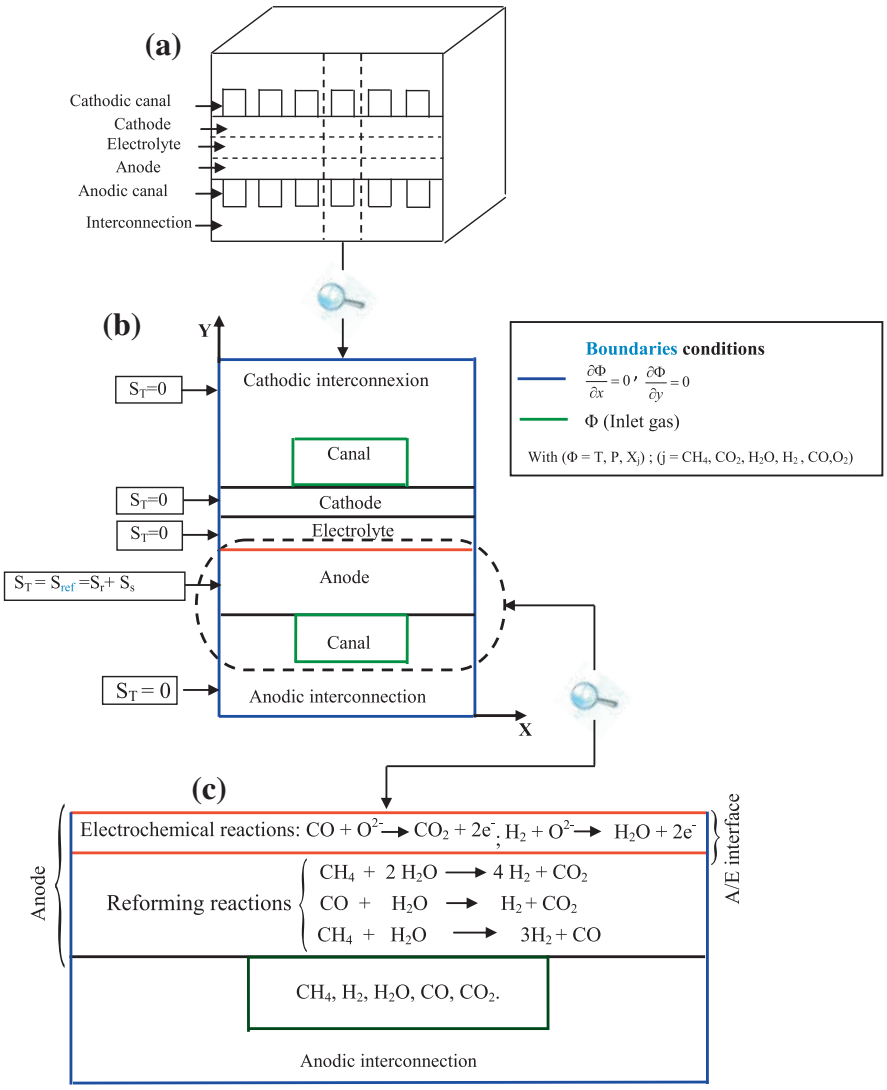

Figure 1 SOFC representative diagram; schematic of a planar SOFC cell (a), physical model and boundary conditions (b), reforming and electrochemical reactions in the anode (c).

Table 2 Coefficients of the equations.

Equations	General variable Φ	Diffusion coefficient Γ_Φ	Source term S_Φ
Mass equation	$\Phi = 1$	$\Gamma_\Phi = 0$	$S_\Phi = 0$
Species equation	$\Phi = Y_j$	$\Gamma_\Phi = (\rho D)_j$	$S_\Phi = S_{Y_j}$
		$\Gamma_\Phi = \kappa.\rho/\mu$	
	With (j = CH_4, CO, CO_2,H_2, O_2, H_2O)		
Pressure equation	$\Phi = P$	$\Gamma_\Phi = \lambda_{(eff,i)}$	$S_\Phi = 0$
Energy equation	$\Phi = T$	With i = (ele, an, cat, int)	$S_\Phi = S_T$

where 'X_j' is the molar fraction of the species 'j'.

So, the gas mixture density can be calculated by (Janardhanan et al., 2007; Hamid, 2010):

$$\rho_{fuel} = \frac{P_{fuel}(M_{CH_4}X_{CH_4} + M_{H_2}X_{H_2} + M_{CO_2}X_{CO_2} + M_{CO}X_{CO} + M_{H_2O}X_{H_2O})}{RT} \quad (10)$$

Noting that the fuel specific heat is defined by (Bertin et al., 1981):

$$Cp_{fuel} = \int_{T_1}^{T_2} \sum X_j Cp_j dT \quad (11)$$

where 'Cp_j' (J kg^{-1} k^{-1}) is the specific heat of species 'j'.

In the energy equation case, the general equation resolution requires the effective thermal conductivity expression ('λ_{eff}' (W m^{-1} K^{-1})) and it can be calculated by the following formula (Zinovik and Poulikakos, 2009; Jiang and Chen, 2009; Pramuanjaroenkij et al., 2010):

$$\lambda_{eff} = \varepsilon\lambda_{fuel} + (1 - \varepsilon)\lambda_{sol} \quad (12)$$

where 'λ_{fuel}' and 'λ_{sol}' are the fuel and the solid thermal conductivity respectively.

The fuel dynamic viscosity is calculated by the following relationship (Hamid, 2010):

$$\mu_{fuel} = \sum_{1}^{5} \mu_j X_j = \mu_{CH_4} X_{CH_4} + \mu_{H_2} X_{H_2} + \mu_{CO_2} X_{CO_2} + \mu_{CO} X_{CO} + \mu_{H_2O} X_{H_2O} \quad (13)$$

For the mass sources, within the anode and the anode/electrolyte interface, the species mass source conservation equation 'S_{Y_j}' is resulting from reforming reactions and electrochemical reactions. In this study, we are interested only in the mass source due to the reforming reactions; the steam reforming reaction '$S_{r,j}$' and water gas shift reaction '$S_{s,j}$' (Wang et al., 2009; Pramuanjaroenkij et al., 2010; Brus and Szmyd, 2008; Iwai et al., 2010). The different mass sources expressions are shown in Table 3. At the cathode, the mass source is the source resulting from oxygen consumption.

$$S_{cat,O_2} = -\frac{M_{O_2}}{2F} i \quad (14)$$

where 'M_{O2}' (kg mol^{-1}), 'i' (A m^2) and 'F' (C mol^{-1}) are the oxygen molar mass, the current density and the faraday's constant.

In this study, the thermal source is the heat source due to the reforming reactions. So the heat source is due to the steam reforming reaction (S_r), which is an endothermic process and the water–gas shift reaction (S_s), which is an exothermic reaction. At the anode, the heat source is described by the following equation (Li et al., 2007; Ho et al., 2010; Kang et al., 2009; Wang et al., 2009; Nikooyeh et al., 2007).

$$S_{T,an} = S_r + S_s \quad (15)$$

With

$$S_r = -R_r \Delta H_r \quad (16)$$

$$S_s = -R_s \Delta H_s \quad (17)$$

'R' (mol m^{-3} s^{-1}) and 'ΔH' (J mol^{-1}) are the reaction rate and reactions enthalpy change (Ivanov, 2007; Brus and Szmyd, 2008; Wang et al., 2009; Zinovik and Poulikakos, 2009).

- Reaction rate expressions

$$R_r = k_r^+ p_{CH_4} p_{H_2O} - k_r^- p_{CO} (p_{H_2})^3 \quad (18)$$

$$R_s = k_s^+ p_{CO} p_{H_2O} - k_s^- p_{CO_2} p_{H_2} \quad (19)$$

Thus, the reaction's rate constants 'k^+' and 'k^-' and the equilibrium constant are:

$$k_r^+ = 2169 \exp(-225103/RT) \quad (20)$$

$$k_s^+ = 0.0183 \exp(-103842/RT) \quad (21)$$

The 'k_r^-'and 'k_s^-' coefficients are determined based on the following equilibrium constants for both reactions.

$$K_{er} = \frac{k_r^+}{k_r^-} \quad (22)$$

$$K_{es} = \frac{k_s^+}{k_s^-} \quad (23)$$

K_{er} and K_{es} equilibrium constants can be calculated by the following empirical equations:

$$K_{er} = 1.0267 \times 10^{10} \exp(-0.2513Z^4 + 0.3665Z^3 + 0.5810Z^2 - 27.134Z + 3.2770) \quad (24)$$

$$K_{es} = \exp(-0.2935Z^3 + 0.6351Z^2 + 4.1788Z + 0.3169) \quad (25)$$

Z: is a variable depending on the temperature (Wang et al., 2009; Iwai et al., 2010; Amornchai et al., 2010).

$$Z = \frac{1000}{T} - 1 \quad (26)$$

Reaction rate Eqs. (18,19) depend on the partial pressure. The 'P_j' of each species ''j'' is equal to its mole fraction 'X_j' multiplied by the total pressure 'P_{fuel}' (Xi et al., 2007; Hamid, 2010).

$$P_j = X_j \, P_{fuel} \quad (27)$$

P_{fuel}: The pressure mixture gas at the inlet channels.

The enthalpies change for the reforming reactions; steam reforming and water–gas shift are given by the following relations:

$$\Delta H_r = 192.220 + 0.0541T - 2.062.10^{-5}T^2 \quad (28)$$

$$\Delta H_s = -44.034 + 0.00847T - 5.819.10^{-7}T^2 \quad (29)$$

The fuel and air physical properties are shown in Table 4. The thermal conductivity, specific heat and the dynamic viscosity of species 'j' are polynomials of temperature of fourth order (CFD Fluent). There expressions are:

$$\lambda_j = a + bT + cT^2 + dT^3 + eT^4 \quad (30)$$

$$Cp_j = a + bT + cT^2 + dT^3 + eT^4 \quad (31)$$

$$\mu_j = a + bT + cT^2 + dT^3 + eT^4 \quad (32)$$

Or, 'a', 'b', 'c', 'd' and 'e' are the empirical constants for each gas. The cell components physical property data are illustrated in Table 5.

Table 3 Mass source expressions resulting from reforming reactions at the anode and the anode/electrolyte interface (Wang et al., 2009; Pramuanjaroenkij et al., 2010; Brus and Szmyd, 2008; Iwai et al., 2010).

Source terms	Species				
	CH_4	H_2	CO_2	CO	H_2O
$S_{r,j}$	$-R_r M_{CH_4}$	$3R_r M_{H_2}$	0	$R_r M_{CO}$	$-R_r M_{H_2O}$
$S_{s,j}$	0	$R_s M_{H_2}$	$R_s M_{CO_2}$	$-R_s M_{CO}$	$-R_s M_{H_2O}$
$S_{ref,j} = S_{r,j} + S_{s,j}$	$-R_r M_{CH_4}$	$(3R_r + R_s) M_{H_2}$	$R_s M_{CO_2}$	$(R_r - R_s) M_{CO}$	$-(R_r + R_s) M_{H_2O}$

Table 4 Fuel and air physical properties.

Physical properties	Species						Refs.
	CH_4	H_2O	H_2	CO_2	CO	O_2	
X_j%	0.29	0.6	0.09	0.01	0.01	/	Li et al. (2008)
M_j [g mol^{-1}]	16	18	2	44	28	32	
D_j [cm^2 s^{-1}]	$D_j = 0.364\left(\frac{T}{273}\right)^{1.5}$					$D_{O_2} = 0.181\left(\frac{T}{273}\right)^{1.5}$	Ferguson et al. (1996)

4. Results and discussion

The results of this study show the thermal fields of an AS_-SOFC under the reforming reactions heat sources effect; the steam reforming reaction heat source effect, the water gas shift reaction heat source effect and the overall reforming reaction heat source effect. Inlet gas temperature and pressure are respectively 1273 K and 3 bars. This analysis is performed at four values (cases) of molar fractions' inlet fuel respectively: (1) CH_4: 0.29, H_2: 0.09, CO_2: 0.01, CO: 0.01, H_2O: 0.6, (2) CH_4: 0.33, H_2O: 0.67, (3) CH_4: 0.01707, H_2: 0.2686, CO_2: 0.0491, CO: 0.024, H_2O: 0.4875 and (4) CH_4: 0.11, H_2: 0.258, CO_2: 0.228, CO: 0.057, H_2O: 0.254. The results are also discussed, following the AS_SOFC temperature elevation and abasement.

4.1. AS_SOFC thermal fields without heat source

Figs. 2 and 3(a and e) present the thermal fields without heat source effect; $S_T = 0$. It is seen that heat transfer channels anode and cathode, warmer environment, to the other SOFC components (anode and cathode interconnections, the cathode, the anode and the electrolyte). For the first, third and fourth cases of fuel molar fractions cited above, the thermal field is constant and the minimum temperature value is 1272.92 K (Fig. 2(a) and Fig. 3(a and e)). In the second case of fuel molar fractions, the minimum temperature value is 1272.84 K which imposes a different distribution to the thermal fields (Fig. 2(e)).

4.2. AS_SOFC thermal fields with effect of steam reforming reaction heat source

Figs. 2 and 3(band f) present the thermal fields with effect of steam reforming reaction heat source; $S_T = S_r$. For all the fuel molar fractions' cases, the minimum temperature value is less than the field minimum temperature value without any heat sources. This minimum temperature is located in the anode far from the channels. Energy consumption is due to the steam reforming reaction endothermicity. This energy consumption is based on the methane percentage in the fuel. A greater methane (CH_4) percentage causes great energy consumption whereas a smaller methane percentage requires low energy consumption. So energy consumption is maximum in the second case of the fuel molar fractions (CH_4: 0.33, H_2O: 0.67), with a $\Delta T = -2.05$ K.

4.3. AS_SOFC thermal fields with effect of water gas shift reaction heat source

Figs. 2 and 3(c and g) present the thermal fields with effect of water gas shift reaction heat source; $S_T = S_s$. For the fuel molar fractions' second case, the thermal field is unchanging. For other fuel molar fractions cases, an increase in the SOFC temperature is distinguished. This increase is located in the anode parts far from the canals. Energy production is due to the water gas shift reaction exothermicity. This energy production is based on the carbon monoxide (CO) percentage in the fuel. A greater carbon monoxide percentage causes a large power generation and a smaller carbon monoxide percentage requires low energy production. So, energy production is maximum at the fuel molar fractions' fourth case ($\Delta T = 12.61$ K) and it is minimum for the fuel molar fractions' second case ($\Delta T = 0$ K).

4.4. AS_SOFC thermal fields with effect of reforming reaction heat source

Figs. 2 and 3(dand h) present the thermal fields with reforming reaction heat source effect; $S_T = S_s + S_r$, which is the sum of two reactions: the steam reforming reaction and the water gas shift reaction. According to the literature review, the Overall reforming reaction is an endothermic reaction. For the first and the second case of the fuel molar fractions, the reaction endothermicity gives a decrease in temperature. The minimum temperature is located at the anode far-away from gas channels (Fig. 2(dand h). Energy consumption is maximum at the fuel molar fractions' second case ($T_{\min} = 1270.79$ K and $\Delta T = -2.05$ K). In contrast, for the fuel molar fractions' third and fourth cases, a SOFC temperature increase is noted. The maximum temperature is focused in the anode away from gas channels (Fig. 3(d and h). This energy production is created by the methane and carbon monoxide content in the fuel. Small methane percentage (third and fourth cases, CH_4: 0.01707 and 0.11), causes the dominance of the exothermic water gas shift reaction.

Table 5 Solid components' physical properties.

Parametres	Anode	Electrolyte	Cathode	Interconnexions	Refs.
κ [m^2]	10^{-12}	10^{-18}	10^{-12}	/	Kang et al. (2009), Zhan et al. (2006), Dokmaingam et al. (2010)
ε [%]	0.4	/	0.5	/	Kang et al. (2009), Zhan et al. (2006)
λ [W m^{-1} K^{-1}]	2	2	2	2	Kang et al. (2009)
e [m]	2.10^{-4}	5.10^{-5}	5.10^{-5}	3.10^{-4}	Wang et al. (2009)

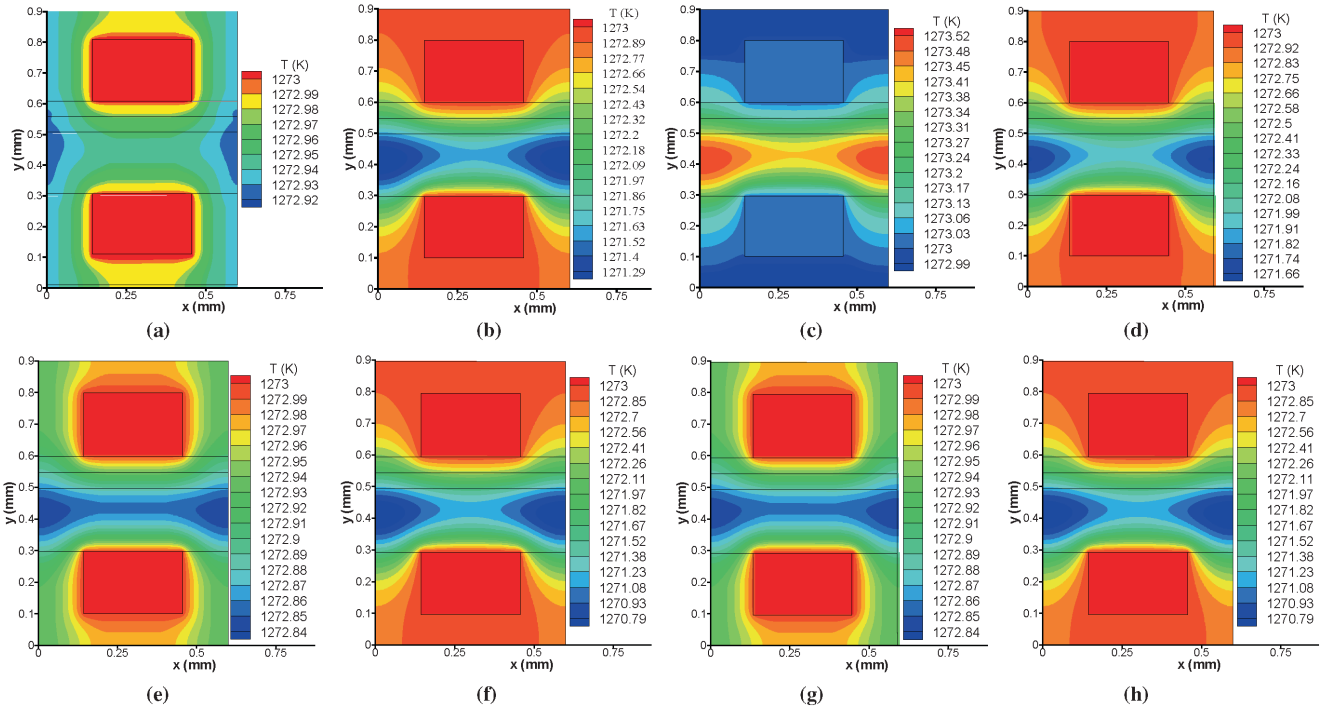

Figure 2 Thermal fields for molar compositions of fuel: CH_4: 0.29, H_2: 0.09, CO_2: 0.01, CO: 0.01, H_2O: 0.6, (a–d) and CH_4: 0.33, H_2O: 0.67, (e–h). Without heat source (a and e), heat source of steam reforming reaction (b and f), Heat source of water–gas shift reaction (c and g), Heat source of overall reforming reaction (d and h).

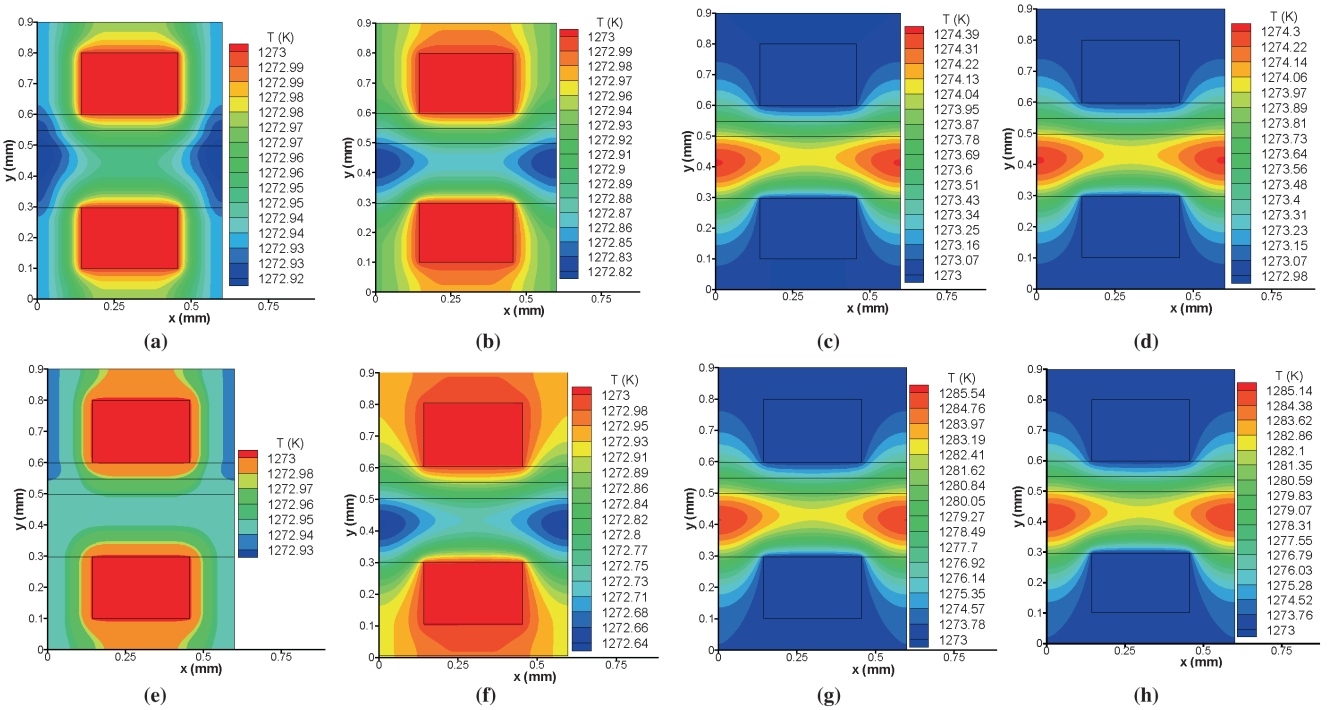

Figure 3 Thermal fields for molar compositions of fuel: CH_4: 0.01707, H_2: 0.2686, CO_2: 0.0491, CO: 0.024, H_2O: 0.4875 (a–d) and CH_4: 0.11, H_2: 0.258, CO_2: 0.228, CO: 0.057, H_2O: 0.254 (e–h). Without heat source (a and e), Heat source of steam reforming reaction (b and f), Heat source of water–gas shift reaction (c and g), Heat source of overall reforming reaction (d and h).

Table 6 contains the maximum and the minimum SOFC temperature (T_{max}, T_{min}) under different heat source influence and the temperature variation (ΔT). The latter is the difference between the SOFC temperature value (T_{max}) under the heat

Table 6 Temperatures and the temperature variations: T_{max}, T_{min}, ΔT.

Heat sources (S_T)	Molar fractions											
	1st Case			2nd Case			3rd Case			4th Case		
	CH4:0.29, H_2:0.09, CO_2:0.01, CO:0.01, H_2O:0.6			CH_4:0.33, H_2O:0.67			CH_4:0.01707, H_2:0.2686, CO_2:0.0491, CO:0.024, H_2O:0.4875			CH_4:0.11, H_2:0.258, CO_2:0.228, CO:0.057, H_2O:0.254		
	T_{max}	T_{min}	ΔT	T_{max}	T_{min}	ΔT	T_{max}	T_{min}	ΔT	T_{max}	T_{min}	ΔT
$S_T = 0$	1273	1272.92	/	1273	1272.84	/	1273	1272.92	/	1273	1272.93	/
$S_T = S_r$	1273	1271.29	−1.63	1273	1270.79	**−2.05**	1273	1272.82	**−0.1**	1273	1272.64	−0.29
$S_T = S_s$	1273.52	1272.99	0.6	1273	1272.84	**0**	1274.39	1273.07	1.47	1285.54	1273	**12.61**
$S_T = S_r + S_s$	1273	1271.66	−1.2	1273	1270.79	**−2.05**	1274.3	1272.98	**1.38**	1285.14	1273	**12.21**

source influence and the SOFC temperature value without heat source (T_{min}). The maximum and the minimum temperature variation values (ΔT) are −0.1, 12.61 and 12.21 K and it is; (−2.05, 0 and −2.05 K) for heat sources due to the steam reforming, water gas shift reaction and the overall reforming reaction respectively. Temperature variation values; 1.38 and 12.21 K show the reforming reaction exothermicity at the fuel molar fractions' third and the fourth cases when methane percent is low in the fuel.

For validation of results, the computed results are compared to our previous results (Abdenebi et al., 2011; Zitouni et al., 2011; Haddad et al., 2013; Oulmi et al., 2011) when the fuel is hydrogen and the chemical reaction is completely exothermic. Temperature field shows a temperature increasing around 10 K. In the present work when the fuel is methane, the chemical reactions studied are the reforming reactions; the steam reforming reaction, the water gas shift reaction and the overall reforming reaction. The temperature low order decrease is reasonable for the endothermic reaction at the SOFC plan studied.

On the one hand, our results are consistent with the mathematical model; the thermal fields under direct reforming reactions effect show a decrease or an increase in temperature value according to the endothermic or exothermic process (steam reforming reaction, overall reforming reaction and water–gas shift reaction). On the other hand, the temperature variation orders under direct reforming reactions are in the same interval as those obtained previously.

5. Conclusion

In this work, the thermal fields' visualization of an AS_SOFC is under inlet gas temperature and pressure values respectively; 1273 K and 3 bars. Results' analysis shows that the reforming heat source effects are based on the inlet fuel molar fractions.

The steam reforming heat source effect is activated by the methane percentage. High methane content in the fuel requires a high energy that is why the steam reforming effect appears .

The temperature decrease is maximum in the fuel molar fractions case when the methane percentage is dominant over the other fuel components ($\Delta T = -2.05$ K) and it is minimum in the fuel molar fractions case when the methane percentage is low ($\Delta T = \pm 0.1$ K).

The water gas shift heat source effect is based on the carbon monoxide percentage. High carbon monoxide content causes an important energy production. As a consequence, the appearance of the water gas shifts the heat source effect. The temperature increase is maximal when the carbon monoxide percentage is highest, ($\Delta T = 12.61$ K, fourth case) and minimum when it is lowest ($\Delta T = 0$ K, second case).

References

Amornchai, Arpornwichanop, Patcharavorachot, Yaneeporn, Assabumrungrat, Suttichai, 2010. Analysis of a proton-conducting SOFC with direct internal reforming. Chem. Eng. Sci. 65, 581–589.

Abdenebi, Hafsia, Bariza, Zitouni, Djamel, Haddad, Hocine, Ben Moussa, Andreadis, George M., Soumia, Abdessemed, 2011. SOFC fuel cell heat production: analysis. Energy Procedia. 6, 643–650.

Bertin, Michel, Faroux, Jean-Pierre, Renault, Jacques, 1981. Thermodynamique, 3th ed. Dunod, Paris.

Brus, Grzegorz, Szmyd, Janusz S., 2008. Numerical modelling of radiative heat transfer in an internal indirect reforming-type SOFC. J. Power Sources 181, 816.

Dokmaingam, P., Irvine, J.T.S., Assabumrungrat, S., Charojrochkul, S., Laosiripojana, N., 2010. Modeling of IT-SOFC with indirect internal reforming operation fueled by methane: effect of oxygen adding as autothermal reforming. Int. J. Hydrogen Energy 35, 13271–13279.

Ferguson, J.R., Fiard, J.M., Herbin, R., 1996. Three-dimensional numerical simulation for various geometries of solid oxide fuel cells. J. Power Sources 58, 109–122.

Haddad, Djamel, Hafsia, Abdenebi, Bariza, Zitouni, Hocine, Ben Moussa, Kafia, Oulmi, 2013. Thermal field in SOFC fed by hydrogen: inlet gases temperature effect. Int. J. Hydrogen Energy 38, 85758583.

Hamid Mounir, 2010. Caractérisation, Modélisation thermo fluide et électrochimique, simulation numérique et étude des performances des nouvelles piles à combustible types IP-SOFC (Integrated-Planar Solid Oxide Fuel Cell) (Doctoral thesis). Univ. Rabat.

Ho, Thinh X., Kosinski, Pawel, Hoffmann, Alex C., Vik, Avrild, 2010. Transport, chemical and electrochemical processes in a planar solid oxide fuel cell: detailed three – dimensional modeling. J. Power Sources 195, 6764–6773.

Ho, Thinh X., Kosinski, Pawel, Hoffmann, Alex C., Vik, Avrild, 2010. Effect of sources on the performance of a planar solid fuel cell. Int. J. Hydrogen Energy 35, 4276–4284.

Hu, Qiang, Wang, Shaorong, Wen, Ting-Lian, 2008. Analysis of processes in planar solid oxide fuel cells. Solid State Ionics 179, 1579–1587.

Ivanov, Peter, 2007. Thermodynamic modeling of the power plant based on the SOFC with internal steam reforming of methane. Electrochim. Acta 52, 39213928.

Iwai, H., Yamamoto, Y., Saito, M., Yoshida, H., 2010. Numerical simulation of intermediate-temperature direct-internal-reforming planar solid oxide fuel cell. Energy 36, 2225–2234.

Janardhanan, Vinod M., Heuveline, Vincent, Deutschmann, Olaf, 2007. Performance analysis of a SOFC under direct internal reforming conditions. J. Power Sources 172, 296307.

Jiang, Tsung Leo, Chen, Ming-Hong, 2009. Thermal-stress analyses of an operating planar solid oxide fuel cell with the bonded compliant seal design. Int. J. Hydrogen Energy 34, 82238234.

Kang, Ying-Wei, Li, Jun, Cao, Guang-Yi, Tu, Heng-Yong, Li, Jian, Yang, Jie, 2009. One-dimensional dynamic modeling and simulation of a planar direct international reforming solid oxide fuel cell. Chin. J. Chem. Eng 17 (2), 304–317.

Kang, Ying-Wei, Li, Jun, Cao, Guang-Yi, Tu, Heng-Yong, Li, Jian, Yang, Jie, 2009. A reduced1D dynamic model of a planar direct internal reforming solid oxide fuel cell. J. Power Sources, 170–176.

Laurencin, J., 2008. Fonctionnement sous méthane d'une pile à combustible «SOFC»: optimisation des performances et de la durabilité. (Doctoral thesis). Inst. Polytechnique de Grenoble.

Li, Jun, Cao, Guang-Yi, Zhu, Xin-Jian, Tu, Heng-Yong, 2007. Two-dimensional dynamic simulation of a direct internal reforming solid oxide fuel cell. J. Power Sources 171, 585–600.

Li, Jun, Kang, Ying-Wei, Cao, Guang-Yi, Zhu, Xin-Jian, Tu, Heng-Yong, Li, Jian, 2008. Nonlinear identification of a DIR-SOFC stack using wavelet networks. J. Power Sources 179, 673–682.

Li, Jun, Kang, Ying-Wei, Cao, Guang-Yi, Zhu, Xin-Jian, Tu, Heng-Yong, Li, Jian, 2008. Numerical simulation of a direct internal reforming sold oxide fuel cell using computational fluid dynamics method. J. Zhejiang Univ. Sci. 9 (7), 961–969.

Nikooyeh, Kasra, Jeje, Ayodeji A., Hill, Josephine M., 2007. 3D modeling of anode-supported planar SOFC with internal reforming of methane. J. Power Sources 171, 601–609.

Oulmi, Kafia, Bariza, Zitouni, Hocine, Ben Moussa, Andreadis, G.M., Hafsia, Abdenebi, 2011. Total polarization effect on the location of maximum temperature value in planar SOFC. Int. J. Hydrogen Energy 36, 4236–4243.

Pramuanjaroenkij, Xiang Yang Zhou, Sadik Kakac, 2010. Numerical analysis of indirect internal reforming with self-sustained electrochemical promotion catalysts. Int. J. Hydrogen Energy. 35, 64826489. CFD Fluent 6.2.16.

Wang, Qiusheng, Li, Lijun, Wang, Cheng, 2009. Numerical study of thermoelectric characteristics of a planar solid oxide fuel cell with direct internal reforming of methane. J. Power Sources 186, 399–407.

Xi, Handa, Sun, Jing, Tsourapas, Vasilios, 2007. A control oriented low order dynamic model for planar SOFC using minimum Gibbs free energy method. J. Power Sources 165, 53266.

Zhan, Zhongliang, Lin, Yuanbo, Pillai, Manoj, Kim, Ilwon, Barnett, Scott A., 2006. High-rate electrochemical partial oxidation of methane in solid oxide fuel cells. J. Power Sources 161, 460–465.

Zinovik, Igor, Poulikakos, Dimos, 2009. Modeling the temperature field in the reforming anode of a button-shaped solid oxide fuel cell. Electrochim. Acta 54, 62346243.

Zitouni, Bariza, Andreadis, G.M., Hocine, Ben Moussa, Hafsia, Abdenebi, Djamel, Haddad, Mostefa, Zeroual, 2011. Two-dimensional numerical study of temperature field in an anode supported planar SOFC: effect of the chemical reaction. Int. J. Hydrogen Energy 36, 4228–4235.